High glucose-induced upregulation of CD36 promotes inflammation stress via NF-κB in H9c2 cells

BAOSHENG HAN[1], JIANZHONG WANG[1], JIAWEI WU[1], FANG YAN[1], YARU WANG[1] and JUN LI[2]

Departments of [1]Cardiac Surgery and [2]Cardiology, Shanxi Cardiovascular Hospital, Taiyuan, Shanxi 030000, P.R. China

Received January 21, 2021; Accepted July 2, 2021

DOI: 10.3892/mmr.2021.12404

Abstract. Cardiac inflammation serves an important role in the progression of diabetic cardiomyopathy. CD36 (cluster of differentiation 36) mediates inflammation stress in a variety of disease states. The present study investigated CD36 expression in high glucose (HG)-induced H9c2 cells, whether CD36 upregulation promotes inflammatory stress, and its potential mechanism. HG induced CD36 expression in a time-dependent manner in cells, which was blocked following CD36 knockout or treatment with N-acetylcysteine or MitoTEMPO. CD36 translocation to the cell membrane was increased at 72 h by HG stimulation of H9c2 cells. Moreover, CD36 knockout inhibited HG-induced reactive oxygen species (ROS) generation, tumor necrosis factor-α, interleukin (IL)-6 and IL-1β expression, and nuclear factor (NF)-κB pathway activation. Further, CD36 knockout reversed metabolic reprogramming, lipid accumulation and AMP-activated protein kinase activation caused by HG. The aforementioned data suggest that HG-induced upregulation of CD36 promotes inflammatory stress via NF-κB in H9c2 cells, mediated by metabolism reprogramming, lipid accumulation and enhanced ROS generation.

Introduction

Diabetic cardiomyopathy (DCM) is a major cardiovascular complication in diabetes that remains the leading cause of mortality in diabetic patients (1). Hyperglycemia is the main clinical manifestation of diabetes, playing a key pathogenic role in the development of DCM (1,2). However, a clear causative role for hyperglycemia has not been established. The major biochemical pathways of hyperglycemic cardiac damage, including chronic hyperglycemia, result in the activation of the inflammatory response and the generation of reactive oxygen species (ROS) (2). Increased inflammatory response influences upstream regulatory events that impair cardiac function and result in cardiomyocyte injury. ROS overproduction subsequently induces injury and an aggressive inflammatory response (3).

Numerous studies have revealed that nuclear factor-κB (NF-κB) is a primary regulator of inflammatory responses; NF-κB is activated in the cardiac myocytes of patients with DCM. Activated NF-κB induces the expression of proinflammatory cytokines, including tumor necrosis factor (TNF)-α, interleukin (IL)-6 and IL-1β, which results in cell infiltration of leucocytes, including macrophages and neutrophils. The NF-κB-dependent mechanism plays a significant role in hyperglycemia-induced myocardial damage and inflammation (2,4). The aforementioned data suggest that inhibition of the inflammatory response by preventing NF-κB pathway activation may have therapeutic potential in DCM.

Cluster of differentiation 36 (CD36), which belongs to a class B scavenger receptor family, is a glycosylated surface receptor present in the cell membrane and in the intracellular compartment of cardiac myocytes (5). High glucose (HG) concentrations can increase *CD36* mRNA translation and subsequently increase CD36 expression in macrophages, renal tubular epithelial cells and dendritic cells (6-8). However, the effects of HG on CD36 in cardiomyocytes have not been demonstrated. Accumulating evidence has focused on the role of CD36: As a fatty acid transporter, it mediates fatty acid uptake, leading to cardiac lipotoxicity and alterations of myocardial energy metabolism (2,5). CD36 is also a signaling molecule that participates in the inflammatory process (9-12). Diverse animal studies have reported that CD36 is important for lipid deposition, and also participates in NF-κB pathway activation and mitochondrial fatty acid oxidation, which contributes to the regulation of chronic metabolic diseases, especially in metabolic disease models that include atherogenic processes and non-alcoholic steatohepatitis (10,13-16). However, studies investigating the effects of CD36 on inflammatory stress in DCM are rare.

The present study investigated CD36 expression in HG conditions, whether CD36 upregulation promotes inflammation stress via NF-κB in HG-induced H9c2 cells, as well as the relevant mechanism.

Correspondence to: Dr Jun Li, Department of Cardiology, Shanxi Cardiovascular Hospital, 18 Yifen Road, Taiyuan, Shanxi 030000, P.R. China
E-mail: lijun097@126.com

Key words: diabetic cardiomyopathy, CD36, reactive oxygen species, H9c2 cells, inflammation

Materials and methods

Reagents and antibodies. Glucose, mannitol, palmitic acid (PA), *N*-acetylcysteine (NAC), MitoTEMPO, and MitoSOX were purchased from Sigma-Aldrich; Merck KGaA. The lentivirus constructs were provided by Shanghai GeneChem Co., Ltd. 2', 7'-Dichlorodihydrofluorescein diacetate (DCFDA) was from Invitrogen (Thermo Fisher Scientific, Inc.). CD36 (cat. no. 14347), NF-κB p65 (cat. no. 8242), inhibitor of κBα (IκBα; cat. no. 4814), AMP-activated protein kinase (AMPK; cat. no. 2532), and phosphorylated (p-)AMPK (cat. no. 4184) antibodies were purchased from Cell Signaling Technology, Inc. Antibodies against β-actin (cat. no. sc-8432) and lamin B (cat. no. sc-374015) were from Santa Cruz Biotechnology, Inc. The TNF-α (cat. no. HSTA00E), IL-6 (cat. no. D6050) and IL-1β (cat. no. DLB50) enzyme-linked immunosorbent assay (ELISA) kits were from R&D Systems.

Cell culture and transfection. H9c2 cells were obtained from American Type Culture Collection and cultured in Dulbecco's modified Eagle's medium (Gibco; Thermo Fisher Scientific, Inc.) with 1 g/l glucose supplemented with 10% fetal bovine serum (Gibco; Thermo Fisher Scientific, Inc.), 100 U/ml penicillin and 100 mg/ml streptomycin at 37˚C in an atmosphere of 5% CO_2. The cells were incubated with normal glucose (NG; 5.6 mM), NG plus mannitol (M; 24.4 mM), HG (30 mM), HG plus NAC (HG + N; 5 mM), and/or MitoTEMPO (HG + T; 10 μM) and HG plus PA (HG + 100 μM PA) for 72 h. The H9c2 cells were infected with LV3 empty vector (LV3-NC), LV3 containing CD36 (LV3-CD36), CD36 knockout short hairpin (sh)RNA (LV3-shRNA) (Shanghai GeneChem Co. Ltd.) lentivirus expression vectors (viral titer: $1x10^9$ transducing U/ml; multiplicity of infection: 10) for 6 h to knockout or overexpress CD36. Thereafter, medium was replaced with fully supplemented DMEM for 24 h, the cells were collected and transduction efficiencies were confirmed by reverse transcription-quantitative PCR. LV3-NC was used as the control group. In the experiment to verify the CD36 shRNA knockout efficiency, scrambled shRNA was used as the control. The sequences of all the shRNAs were as follows: CD36-RNAi (10899-1), 5'-CCGACGTTAATCTGAAAG GAA-3'; CD36-RNAi (10900-1), 5'-GCCATAATCGACAC ATATAAA-3'; CD36-RNAi (10902-1), 5'-CCATTGGTG ATGAGAAGGCAA-3'; scrambled shRNA, 5'-TTCTCCGAA CGTGTCACGT-3'. LV3-CD36: CD36 (64809-1)-p1, 5'-GAA CCGTCAGATCCGCTAGCCGCCACCATGGGCTGTGAC CGGAACTG-3'; CD36 (64809-1) -p2, 5'-GGAGGGAGA GGGGCGGATCTTATTTTATTGTTTTCGATCTGC-3'. The H9c2 cells were designated the empty vector control group (NC), high-CD36 expression group (HC) and CD36 knockout group (KC).

Western blotting. Total protein was extracted from the H9c2 cells using radioimmunoprecipitation assay buffer (Boster Biological Technology); nuclear and cytoplasmic proteins were extracted using a commercial nucleoprotein extraction kit (cat. no. 40010) referring to the manufacturer's instructions (Active Motif, Inc.). Western blotting was performed according to a previous publication (17). The primary antibodies (CD36, NF-κB p65, IκBα, AMPK, p-AMPK, β-actin, lamin B) were diluted 1:1,000; goat anti-rabbit (cat. no. SA00001-2; ProteinTech Group, Inc.) or mouse IgG horseradish peroxidase conjugated antibodies (cat. no. SA00001-1; ProteinTech Group, Inc.) were diluted 1:5,000. The results were scanned using the Odyssey Fc System (LI-COR Biosciences). The intensity of the bands was measured using LabWorks 4.5 (Analytik Jena AG).

Reverse transcription-quantitative PCR (RT-qPCR). Total RNA and complementary DNA (cDNA) synthesis from H9c2 cells were prepared using TRIzol® (Invitrogen; Thermo Fisher Scientific, Inc.) and RevertAid reverse transcription kits (Invitrogen; Thermo Fisher Scientific, Inc.) according to the manufacturer's instructions. Real-time PCR was performed on an Agilent Mx3000P QPCR System using SYBR Premix Ex Taq™ II (Takara Biotechnology Co., Ltd.) at default thermal cycling conditions: 2 min at 50˚C, 10 min at 95˚C, followed by 40 cycles of 15 sec at 95˚C for denaturation and 1 min at 60˚C for annealing and extension. The expression levels were represented by the comparative threshold cycle value ($2^{-\Delta\Delta Cq}$) (18) and normalized to β-actin. The primers used were as follows: CD36 sense, 5'-ATAACTGGATTCACTCTACAGTTTGC-3' and antisense, 5'-GATCTGCAAGCACAGTATGAAATC-3'; TNF-α sense, 5'-GATCGGTCCCAACAAGGAGG-3' and antisense, 5'-TTTGCTACGACGTGGGCTAC-3'; IL-6 sense, 5'-CCACCCACAACAGACCAGTA-3' and antisense, 5'-ACA GTGCATCATCGCTGTTC-3'; IL-1β sense, 5'-GAAGAATCT ATACCTGTCCT-3' and antisense, 5'-CTTTTCCATCTTCTT CTTTG-3'; and β-actin sense, 5'-CCCTAAGGCCAACCG TGAAAAG-3' and antisense, 5'-TACGTACATGGCTGG GGTGT-3'.

Detection of ROS. Intracellular ROS were measured using DCFDA. H9c2 cells were seeded into 6-well plates at a density of $1.5x10^6$ cells/ml and incubated under different experimental conditions for 72 h. After culturing, H9c2 cells were incubated in 10 μM DCFDA at 37˚C for 30 min in the dark, and then washed three times with warm buffer. Mitochondrial ROS (mtROS) were detected using MitoSOX, a specific mitochondria-targeted superoxide fluorescent probe. H9c2 cells were incubated with a 5-μM MitoSOX working solution at 37˚C for 30 min before flow cytometry. The measurement of intracellular and mtROS was performed using flow cytometry (FACSCalibur; BD Immunocytometry Systems), and the analysis was performed using FlowJo software (version 10; FlowJo LLC).

ELISA. After cells were cultured in 6-well plates for 72 h, the supernatants were collected. TNF-α, IL-6 and IL-1β protein levels in the culture supernatants were detected using a commercial ELISA kit according to the manufacturer's instructions (Nanjing Jiancheng Bioengineering Institute).

Immunofluorescence. H9c2 cells were cultured and stimulated in 6-well chamber slides under different experimental conditions for 72 h, then fixed in frozen acetone for 20 min at 4˚C, then the cells were incubated in 0.1% Triton X-100 for 20 min at room temperature to permeabilize the cell membrane. The cells were blocked with 5% bovine serum albumin (cat. no. SW3015; Beijing Solarbio Science & Technology Co.,

Ltd.) for 30 min, and incubated with antibodies (anti-NF-κB p65, 1:50, cat. no. 8242; anti-CD36, 1:50, cat. no. 14347; Cell Signaling Technology, Inc.) overnight at 4˚C. Then, the cells were exposed to FITC-conjugated secondary antibody (1:200; cat. nos. 31461; Invitrogen, Thermo Fisher Scientific, Inc.) for 1 h at 37˚C. The cells were counterstained with 4',6-diamidino-2-phenylindole for 5 min at room temperature. Images were captured using a fluorescence microscope (magnification, x400; Olympus BX63; Olympus Corporation) or confocal microscope (magnification, x400; Olympus FV 1000 Viewer).

Extracellular flux assay. H9c2 cells were seeded at a density of 50,000-80,000 cells/well in specialized XF96 cell culture microplates (Seahorse Bioscience; Agilent Technologies, Inc.). The cells were exposed to different conditions for 72 h at 37˚C. Then, the medium was replaced with Seahorse running medium (XF base medium supplemented with 10% D-glucose, 100 mM pyruvate and 200 mM glutamine for the mitochondrial stress test, or with 200 mM glutamine alone for the glycolysis stress test). Subsequently, incubation was performed in a non-CO_2 incubator for 60 min at 37˚C. The basal oxygen consumption rate and extracellular acidification rate were recorded for 24 min, followed by performance of the mitochondrial stress test (1 μM oligomycin, 2 μM trifluoromethoxy carbonylcyanide phenylhydrazone and 0.5 μM rotenone/antimycin A) and glycolysis stress test (10 mM glucose, 1 μM oligomycin, and 50 mM 2-DG). Subsequently, the cells were lysed in RIPA buffer and subjected to the Bradford protein assay (Bio-Rad Laboratories, Inc.). The oxygen consumption rate (OCR) and extracellular acidification rate (ECAR) values were normalized by the protein values in each well.

Quantitative detection of triglycerides. In total, 4-5 million H9c2 cells were collected, sonicated by ultrasonication (200 W; 20 KHz, pulse 20%; run for 2 sec, stop 1 sec) for 1 min, then centrifuged at 8,000 x g for 10 min at 4˚C, and the supernatant was retained for detection. The triglyceride content was measured according to the manufacturer's instructions (cat. no. A110-1-1; Nanjing Jiancheng Bioengineering Institute).

Statistical analysis. The statistical significance of differences among groups was analyzed using one-way analysis of variance, followed by post hoc testing using the Tukey-Kramer method. All experiments were performed at least three times. $P<0.05$ was considered to indicate a statistically significant difference. Data were expressed as the mean ± standard deviation (SD).

Results

HG-induced CD36 expression is partially dependent on ROS in H9c2 cells. To determine the effect of HG on CD36 expression *in vitro*, H9c2 cells were incubated with high concentrations of glucose, and the CD36 mRNA and protein levels were examined. HG induced a time-dependent increase in CD36 expression in the cells (Fig. 1A and B). CD36 mRNA and protein expression was increased within 12 h and continued to increase up to 72 h. CD36 is a fatty acid transport protein; its function mainly depends on its location in the cell membrane (12). Thus, the translocation of CD36 to the cell membrane in HG-treated H9c2 cells was next evaluated by immunofluorescence staining observed by confocal microscopy. As shown in Fig. 1C, fluorescence of CD36 was low at 0 h. HG stimulation for 72 h resulted in increased fluorescence of CD36. In the 0-h group, the fluorescence was distributed in the cytoplasm of H9c2 cells; however, in the 72-h HG-stimulated group, the fluorescence tended to be distributed around the cell membrane. Flow cytometry analysis revealed that the levels of CD36 in the cell membrane were higher at 24 and 72 h compared with 0 h (Fig. 1D).

Next, it was assessed whether ROS mediated the HG-induced CD36 expression in the H9c2 cells. ROS generation was detected by the cellular ROS indicator DCFDA. Following the addition of HG, ROS production was increased (Fig. 1E). Mannitol treatment did not affect CD36 expression (Fig. 1F); NAC (an intracellular ROS scavenger) and MitoTEMPO (a mitochondria-targeting antioxidant) significantly decreased HG-induced generation of ROS (Fig. 1E). The addition of NAC or MitoTEMPO inhibited the HG-induced CD36 protein overexpression significantly (Fig. 1G).

Knockout of CD36 prevents NF-κB-mediated inflammatory responses and ROS generation in HG induced-H9c2 cells. It was investigated whether inhibition of CD36 expression could prevent cellular damage in H9c2 cells by modulating the inflammatory responses. Lentivirus vectors (LV3-shRNA) were constructed to knock down CD36 expression, which was validated by RT-qPCR (Fig. 1H). Following 72-h exposure to HG or HG + control empty vector conditions, TNF-α, IL-6 and IL-1β mRNA and protein levels in the cells were significantly enhanced, whereas knockout of CD36 alleviated these changes (Fig. 2A and B). Subsequently, the changes in the key transcription factor NF-κB were assessed. The increased nuclear levels of the p65 subunit of NF-κB and decreased levels of IκBα were used to represent the activation of NF-κB signaling. Nuclear levels of NF-κB p65 were increased and cytosolic levels of IκBα were decreased in H9c2 cells incubated with HG or HG + C for 72 h compared with that in cells incubated with NG (Fig. 2C-E). CD36 shRNA reversed these changes. The results of immunofluorescence detection of NF-κB p65 (Fig. 2F) were consistent with the results showing that knockout of CD36 inhibited NF-κB activation in HG-treated H9c2 cells.

Next, the effect of CD36 on HG-induced ROS production was determined. Intracellular ROS levels were examined using DCFDA. Flow cytometry showed increased fluorescence in the HG group compared with the NG group, and CD36 knockout significantly inhibited HG-induced ROS (Fig. 2G).

Knockout of CD36 prevents NF-κB by inhibiting ROS, and mitochondrial ROS plays a major role. ROS is one of the important activators of NF-κB (4). Next, it was determined whether CD36 activates NF-κB through ROS. H9c2 cells were transfected by lentivirus vector to overexpress CD36 before HG stimulation. The CD36-overexpressing cells had increased nuclear levels of NF-κB p65 and decreased cytosolic levels of IκBα, which were blocked by MitoTEMPO (Fig. 3A-C). The results of immunofluorescence detection of NF-κB p65 (Fig. 3D) were consistent with the western blotting results.

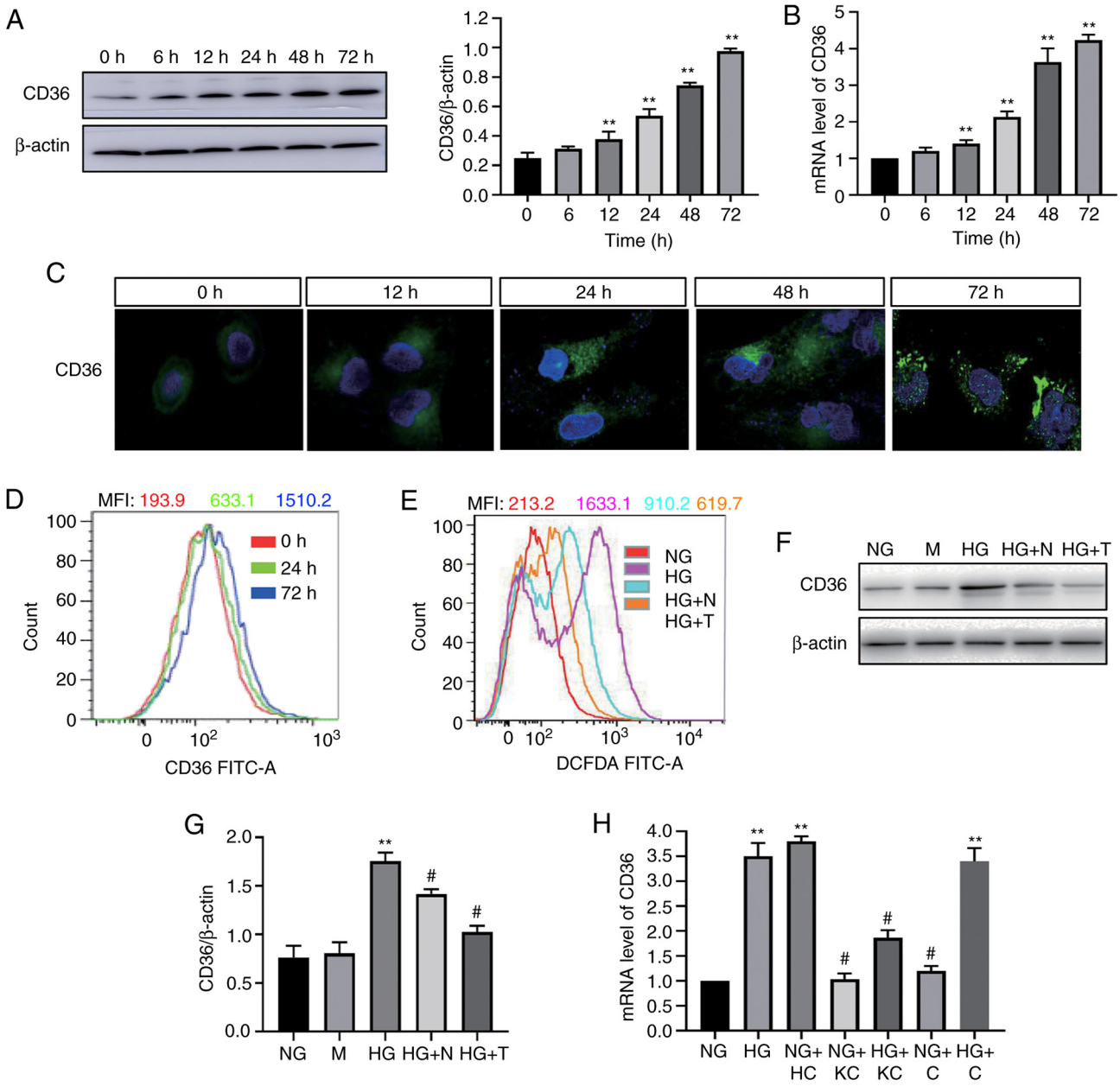

Figure 1. HG-induced CD36 expression in H9c2 cells is dependent on reactive oxygen species. CD36 expression was determined by western blotting (A) and reverse transcription-quantitative PCR (B) in HG-treated cells. (C) CD36 levels in the cell membrane were measured by immunofluorescence staining in HG-treated cells (magnification, x400). (D) CD36 levels in the cell membrane were measured by flow cytometry. (E) Quantitative analysis of DCFDA fluorescence intensity using flow cytometry. (F and G) CD36 expression levels were analyzed by western blotting. (H) mRNA expression levels of CD36 were measured by reverse transcription-quantitative PCR. H9c2 cells were incubated with NG (5.6 mM, NG group), NG plus mannitol (24.4 mM, M group), HG (30 mM, HG group), HG plus N-acetylcysteine (5 mM, HG + N group) and HG plus MitoTEMPO (10 μM, HG + T group) , NG plus LV3 containing CD36 (NG + HC group), NG plus LV3 containing CD36 knockout (NG + KC group), HG plus LV3 containing CD36 knockout (HG + KC group), NG plus LV3 empty vector (NG + C group) and HG plus LV3 empty vector (HG + C group) for 72 h. Data are expressed as the means ± SD. n=4. **P<0.01 vs. NG or 0 h; $^{\#}$P<0.05 vs. HG. HG, high glucose; NG, normal glucose; DCFDA, 2', 7'-dichlorodihydrofluorescein diacetate.

To further demonstrate the role of mtROS in this pathway, the mtROS level was detected using the specific mitochondria-targeted superoxide fluorescent probe MitoSOX. As shown in Fig. 3E, CD36 knockout significantly inhibited HG-induced mtROS, by ~50% at 72 h. These data support for a critical role of mtROS in CD36-induced NF-κB activation in H9c2 cells.

Knockout of CD36 ameliorates metabolism reprogramming and lipid accumulation caused by HG in H9c2 cells. It has previously been demonstrated that mtROS production is associated with altered bioenergetics (3). Therefore, the present study investigated the effects of HG on metabolism reprogramming by treating H9c2 cells with HG for 72 h, then subjecting them to extracellular flux analysis, which measures the OCR and ECAR (Fig. 4A). Basal respiration was unchanged in the HG or HG + C groups when compared with the NG group, but ATP production and maximal respiration were significantly decreased after HG treatment (Fig. 4B). Non-mitochondrial respiration and proton leak were increased in response to HG

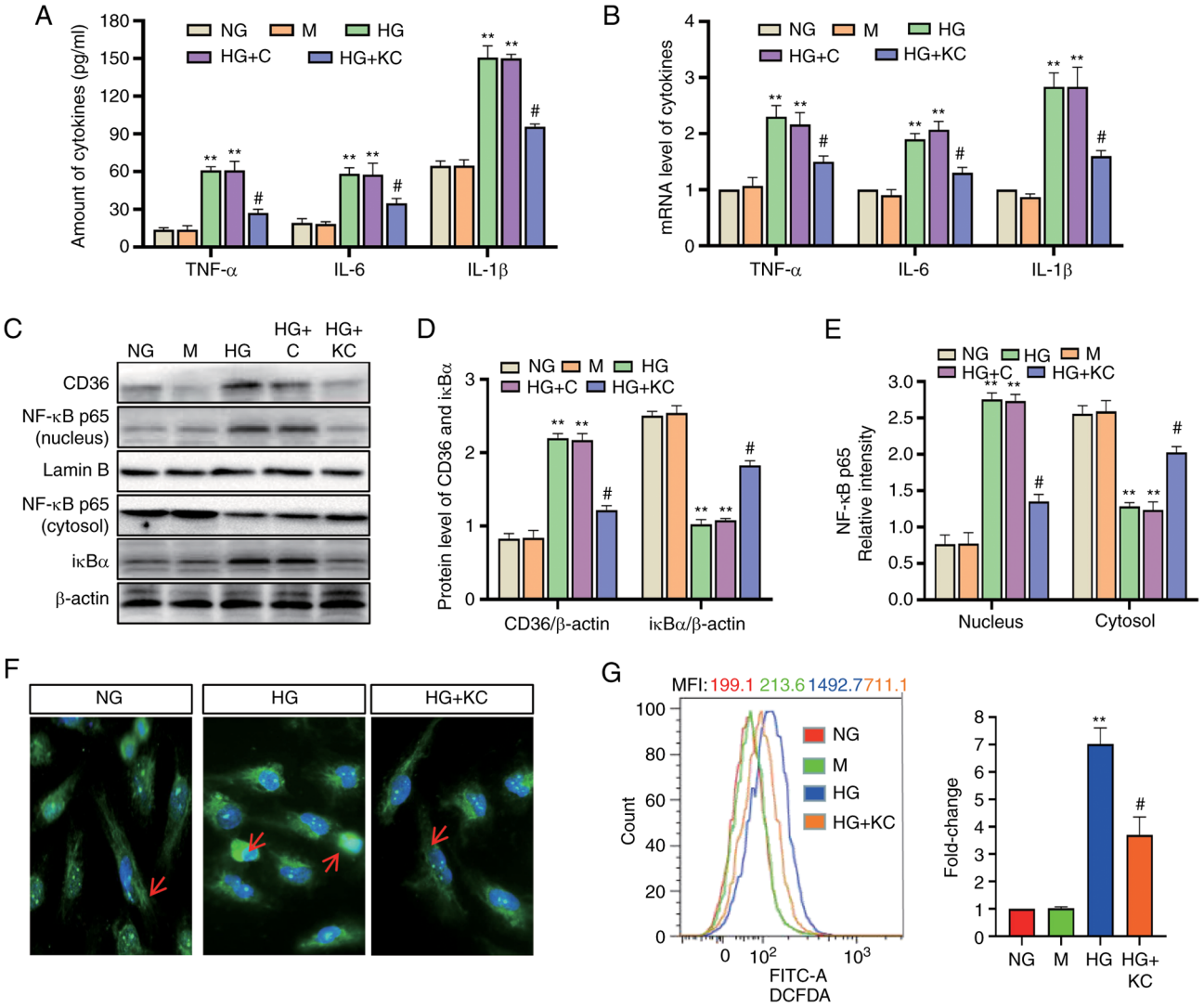

Figure 2. Knockout of CD36 prevents NF-κB-mediated inflammatory responses and ROS generation in HG-induced H9c2 cells. H9c2 cells were incubated with NG (5.6 mM, NG group), NG plus mannitol (24.4 mM, M group), HG (30 mM, HG group), HG plus LV3 empty vector (HG + C group) or HG plus LV3 containing CD36 mutant (HG + KC group) for 72 h. (A) The TNF-α, IL-6 and IL-1β levels in the culture supernatant were measured by enzyme-linked immunosorbent assay. (B) The mRNA levels of TNF-α, IL-6 and IL-1β were measured by reverse transcription-quantitative PCR and normalized to β-actin. (C and D) CD36 in the nucleus and cytosol and nuclear translocation of NF-κB p65 protein were detected by western blotting. (C and E) IκBα protein in cytosolic extracts was measured by western blotting. (F) Immunofluorescence labeling with anti–NF-κB p65 (magnification, x400). (G) Intracellular ROS were detected by flow cytometry. Data are expressed as the means ± SD. n=4. **P<0.01 vs. NG; $^{\#}$P<0.05 vs. HG. NF-κB, nuclear factor-κB; ROS, reactive oxygen species; HG, high glucose; NG, normal glucose; TNF, tumor necrosis factor; IL, interleukin.

treatment. Knockout of CD36 attenuated the OCR changes caused by HG.

The H9c2 cells in the NG group had a low ECAR, consistent with low glycolytic metabolism. HG or HG + C treatment for 72 h induced elevation in the ECAR, consistent with an increase in glycolysis (Fig. 4C). Given the existence of glucose and lipid metabolism disorder in DCM, ECAR changes were also measured in H9c2 cells treated with HG plus PA (100 μM; HG + PA). HG + PA treatment induced a decreased ECAR, consistent with a metabolic switch to fatty acid oxidation (Fig. 4D). Knockout of CD36 reversed the ECAR changes caused by HG (Fig. 4D), but similar responses were not observed when transfected with empty vector.

To elucidate the mechanisms by which CD36 regulates fatty acid oxidation metabolism, the levels of lipid accumulation and fatty acid oxidation-related pathway were examined in the H9c2 cells. The cellular triglyceride content in the HG or HG + C group, which was significantly higher than that in the NG group, could be partially reversed by knockout of CD36 (Fig. 4E). Further, the level of AMPK phosphorylation was measured, which was a key regulator in the maintenance of cellular fatty acid homeostasis and controls fatty acid β-oxidation in mitochondria (19), with western blotting. HG treatment for 72 h induced a decline in p-AMPK protein in the H9c2 cells (Fig. 4F). Knockout of CD36 prevented these alterations, as compared with the HG group, but similar effects were not observed in the HG + C group.

Discussion

The present study demonstrated that HG can upregulate CD36 at mRNA and protein levels in H9c2 cells, which was partially

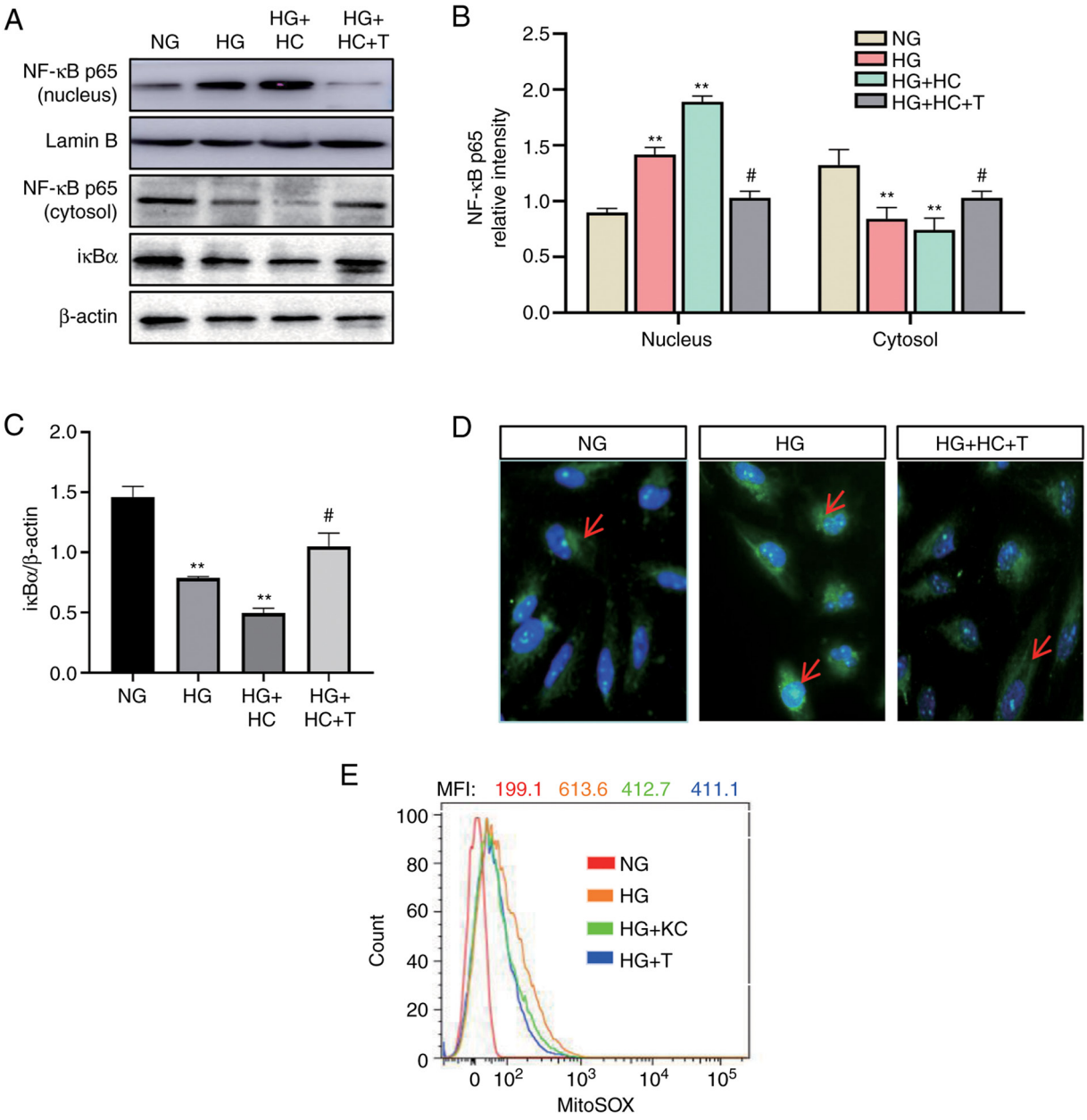

Figure 3. Knockout of CD36 prevents NF-κB by inhibiting ROS in H9c2 cells. H9c2 cells were incubated with NG (5.6 mM, NG group), HG (30 mM, HG group), HG plus LV3 empty vector (HG + C group), HG plus LV3 containing CD36 (HG + HC group), HG + HC plus MitoTEMPO (100 nM, HG + HC + T group), HG plus LV3 containing the CD36 short hairpin RNA (HG + KC group), and HG plus MitoTEMPO (10 μM, HG + T group) for 72 h. (A and B) The nuclear translocation of NF-κB p65 protein in the nucleus and cytosol was detected by western blotting. (A and C) The IκBα protein expression in cytosolic extracts was measured by western blotting. (D) Immunofluorescence labeling with anti-NF-κB p65 (magnification, x400). (E) Expression levels of mitochondrial ROS were detected by FACS using MitoSOX reagent. Data are expressed as the mean ± SD. n=4. **P<0.01 vs. NG; $^{\#}$P<0.05 vs. HG. NF-κB, nuclear factor-κB; ROS, reactive oxygen species; HG, high glucose; NG, normal glucose.

dependent on ROS generation. Knockout of CD36 attenuated HG-induced activation of NF-κB signaling. It was further demonstrated that the underlying molecular mechanisms may be due to inhibited mitochondrial ROS production, changes in metabolism and decreased lipid deposition.

CD36, a membrane glycoprotein, serves an important role in DCM. The main mechanism is that, as a fatty acid transporter, CD36 mediates fatty acid transport, promoting fatty acid oxidation and leading to cardiac lipotoxicity and altered myocardial energy metabolism (2). Two major signaling pathways for regulating CD36 in DCM have been explored: Insulin levels and the energy demand of the heart (20). However, some studies have also found that sarcolemmal CD36 levels in cardiac muscle are increased in type 1 DCM, in which plasma insulin levels are greatly decreased or absent, suggesting that in addition to insulin levels (20-22), hyperglycemia may have a regulatory effect on CD36 expression. Hyperglycemia can upregulate CD36 protein and mRNA expression in macrophages (6). In HG-treated HK-2 cells, the levels of *CD36* mRNA transcripts and subsequent protein translation were increased in a time-dependent manner (7). Consistently, it was found that exposure to HG induced significantly increased CD36 expression in H9c2 cells. However, CD36 is present not only at the cell surface but is also found in endosomes,

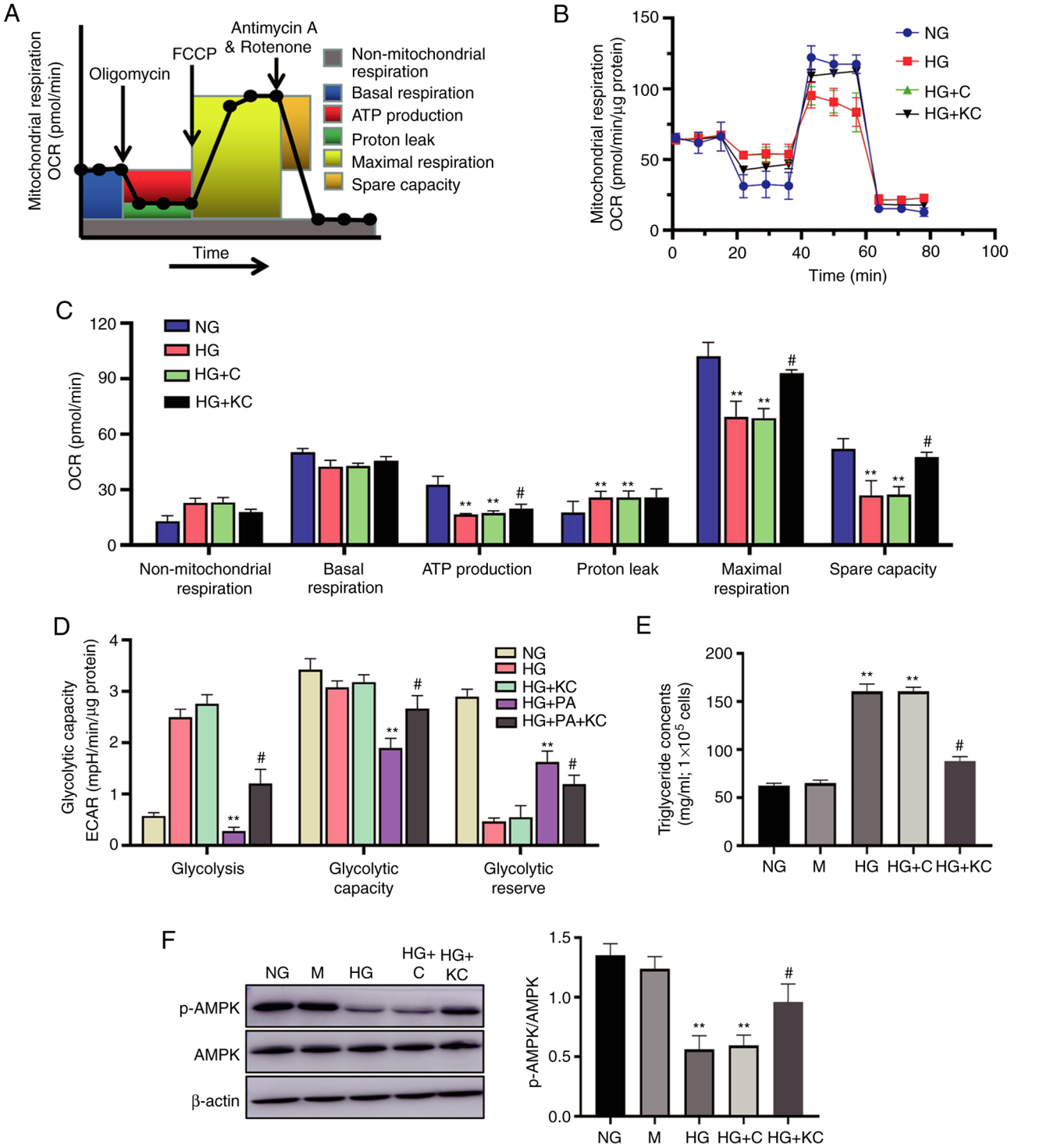

Figure 4. Knockout of CD36 ameliorates metabolism reprogramming and lipid accumulation caused by HG in H9c2 cells. H9c2 cells were incubated with NG (5.6 mM, NG group), HG (30 mM, HG group), HG plus LV3 containing CD36 mutant (HG + KC group), HG plus PA (100 μM HG + PA group), or HG + PA plus LV3 containing CD36 mutant (HG + PA + KC group) for 72 h. (A) Protocol used in data collection and calculations for evaluating mitochondrial respiration. (B) Representative OCR curve. (C) Quantitative analysis of non-mitochondrial respiration, basal respiration, ATP production, proton leak, maximal respiration and spare respiratory capacity. (D) Quantitative analysis of glycolysis, glycolytic capacity and glycolytic reserve. All measured OCR and ECAR were normalized by total cellular protein. (E) The triglyceride content in the cells. (F) The p-AMPK and AMPK expression levels were analyzed by western blotting. Data are expressed as the mean ± SD. n=4. **P<0.01 vs. NG, $^{\#}$P<0.05 vs. HG. HG, high glucose; OCR, oxygen consumption rate; ECAR, extracellular acidification rate; p-, phosphorylated-.

the endoplasmic reticulum and the mitochondria. CD36 can migrate between these locations via vesicular transport along exocytotic and endocytic pathways to control lipid homeostasis and energy reprogramming (12). There is subcellular localization of CD36 in cardiomyocytes (23). CD36 is a fatty acid transporter, and its main role depends on the amount localized in the cell membrane (12). Therefore, in the present study, the total protein expression of CD36 was first detected

in H9c2 cells induced by HG, and the localization of CD36 was then observed in cells with a confocal microscope. The results show that CD36 fluorescence was distributed in the cytoplasm of H9c2 cells in the 0-h groups. However, CD36 fluorescence tended to be distributed around the cell membrane in the 72-h groups. To quantify CD36 expression in the cell membrane, flow cytometry was used (which mainly detects cell surface proteins). The flow cytometry results are consistent with that of the western blotting. It was also found that at early-stage stimulation by HG for 24 or 48 h, CD36 localization in the cell membrane of H9c2 cells was increased, but not significantly, while it was increased at 72 h. H9c2 cell responses to a HG environment first involve an increased ATP/AMP ratio, which results in AMPK inactivation. AMPK inactivation may inhibit the membrane translocation of CD36 (16,24). However, persistent HG can contribute to cardiomyocyte damage, such as oxidative stress, mitochondrial dysfunction and the activation of several signaling molecules (2). All of these may have the effect of increasing CD36 expression and membrane translocation in H9c2 cells. ROS generation induces CD36 expression in other cell types (7,25). Further, the present data show that MitoTEMPO or NAC can decrease CD36 overexpression in HG-induced H9c2 cells, suggesting that there may be crosstalk between ROS and the CD36 pathway in HG-treated H9c2 cells.

CD36 is not only a fatty acid transporter, but also a signaling molecule involved in inflammatory responses in a variety of disease states (7-16). In atherogenic processes, CD36 is important for activating the NLRP3 (NLR family pyrin domain containing 3) inflammasome and the NF-κB pathway (9,10). In non-alcoholic steatohepatitis, knockout of CD36 decreased inflammation via the NF-κB pathway inactivation (16). NF-κB is a primary regulator of inflammatory responses, and serves an important role in the development of DCM. Activated NF-κB can induce the expression of proinflammatory cytokines, including TNFα, IL-6 and IL-1β. These cytokines perform an important stress response in myocardial injury (2). In the present study, knockout of CD36 prevented inflammatory responses in HG-induced H9c2 cells. The mechanism that affected this involved the restoration of abnormal activation of the NF-κB system. These results certainly warrant further study of the mechanism of activation of NF-κB by CD36. Previous studies have confirmed that ROS is an important activator of NF-κB (26-28). The results of the present study indicate that when MitoTEMPO was used to inhibit ROS production, NF-κB activation by CD36 overexpression was significantly suppressed. These data provide clear evidence that ROS may play an important role in CD36 activation of the NF-κB pathway in HG-induced injury and inflammation in H9c2 cells. As a membrane fatty acid transporter, CD36 mediates fatty acid transport, leading to increased intracellular lipid deposition in a variety of disease states, causing mitochondrial damage via increased ROS production and cellular inflammation. Additionally, CD36 is a cell transduction protein that activates multiple signaling pathways (10,12,23,29). Thus, it is believed that, in cardiomyocytes, the increased CD36 expression induced by HG also acts both ways. Therefore, both CD36-induced lipid deposition and NF-κB inflammatory signaling pathway activation were detected. The results indicated that CD36-induced intracellular lipid deposition and inflammatory signaling pathway activation plays a role in DCM.

ROS production is closely associated with mitochondrial metabolism. Numerous studies have found that metabolic remodeling, increased lipid utilization and decreased glucose metabolism play a role in the development of DCM 1-3. The present study examined the metabolic changes in cultured H9c2 cells under HG stimulation. HG decreased the levels of oxidative phosphorylation and induced the elevation of glycolysis in H9c2 cells, as demonstrated by extracellular flux analysis. The base ECAR represents the non-glycolytic acid production of the cell; the ECAR after the addition of glucose represents the glycolytic capacity of the cells at the time. With the addition of the oligomycin, oxidative phosphorylation was inhibited, and the cells were supplied with oxygen by glycolysis. At this point, acid production increases, and the increased ECAR represents the cell's remaining glycolytic capacity, or potential; the total value represents the maximum glycolytic capacity of the cell. Finally, a glycolytic inhibitor is added, and the ECAR after the addition of this drug represent acid production beyond glycolysis; this can be due to a lack of mitochondrial respiration (30). The 72-h HG treatment induced ECAR elevation; knockout of CD36 reversed the ECAR, promoting mitochondrial respiration. In addition, there are complex metabolic disorders of hyperglycemia and hyperlipidemia on a whole-body level. It was also found that in HG and high PA conditions, H9c2 cells begin to rely on fatty acid oxidation for energy production, similar to the metabolic remodeling *in vivo*. Knockout of CD36 protected H9c2 cells from the imbalance of energy homeostasis and lipid accumulation caused by HG, indicating that the metabolic disturbance caused by HG may partly be due to CD36.

AMPK regulates fatty acid oxidation, and has emerged as a potential therapeutic target for various metabolic disorders, including diabetes mellitus (31). In non-alcoholic steatohepatitis, CD36 regulates AMPK activation via the phosphorylation of LKB1 (serine/threonine kinase 11) (16). In skeletal muscle, exercise regulates AMPK activation partly through CD36 (32). AMPK activation was decreased in diabetic nephropathy, neuropathy and retinopathy (33). Nevertheless, in the present study, AMPK activation was significantly decreased in H9c2 cells that had been stimulated by HG for 72 h. CD36 is a well-known cell membrane protein and has been studied extensively in cardiomyocytes; however, current studies have focused on the role of CD36 as a fatty acid transporter (34). The association between CD36 and fatty acid oxidation, as well as CD36-induced cellular inflammation and cell metabolism, has not been clarified. Previous studies have found that CD36 can inhibit AMPK activation, which has been confirmed in liver cells and macrophages (16,32,35). Therefore, the association between CD36 and AMPK in cardiomyocytes was further investigated. The knockout of CD36 can improve AMPK inactivation by HG. The results suggest an association between CD36 and AMPK in H9c2 cells. However, the relevant mechanism still requires further research and confirmation.

However, a few limitations of the present study should be addressed. Firstly, HG-stimulated H9c2 cells were used to simulate a diabetic renal tubular injury model *in vitro*. This cell model was used based on previous research (36-38). However, there have been several studies on H9c2 cells as a model in

DCM (36-39). H9c2 cells are derived from rat cardiomyocytes and differ from primary cardiomyocytes; human cardiomyocytes or primary cardiomyocytes would represent a better model. Relevant *in vivo* studies will be conducted later, which should be more appropriate. Secondly, previous studies have reported that CD36 mediates ROS production (7,25,40); inhibiting intracellular ROS decreased CD36 expression (7,25). However, this is unclear in cardiomyocytes. The present study only proves that the association between CD36 and ROS and HG-induced CD36 expression in H9c2 cells relies partially on ROS.

In conclusion, HG can increase CD36 expression, which leads to the activation of NF-κB signaling. This effect is mediated by metabolism reprogramming and lipid accumulation, resulting in enhanced ROS generation.

Acknowledgements

Not applicable.

Funding

The present study was supported by the grant from Shanxi Cardiovascular Hospital (grant no. XYS20200101).

Availability of data and materials

All data generated or analyzed during the present study are included in this article.

Authors' contributions

BH and JL designed the study. JWa supervised the entire project and conducted analyses of western blotting images. BH wrote the manuscript. BH and JL performed most of the experiments and data analysis. JWu analyzed the western blot images. FY contributed to data analysis. YW assisted with the experiments and manuscript preparation. BH and JL confirm the authenticity of all the raw data. All authors reviewed the data and read and approved the final version of the manuscript.

Ethics approval and consent to participate

Not applicable.

Patient consent for publication

Not applicable.

Competing interests

The authors declare that they have no competing interests.

References

1. Falcão-Pires I and Leite Moreira AF: Diabetic cardiomyopathy: Understanding the molecular and cellular basis to progress in diagnosis and treatment. Heart Fail Rev 17: 325-344, 2012.
2. Jia G, Hill MA and Sowers JR: Diabetic cardiomyopathy: An update of mechanisms contributing to this clinical entity. Circ Res 122: 624-638, 2018.
3. Kaludercic N and Di Lisa F: Mitochondrial ROS formation in the pathogenesis of diabetic cardiomyopathy. Front Cardiovasc Med 7: 12, 2020.
4. Jia G, DeMarco VG and Sowers JR: Insulin resistance and hyperinsulinaemia in diabetic cardiomyopathy. Nat Rev Endocrinol 12: 144-153, 2016.
5. Brinkmann JF, Abumrad NA, Ibrahimi A, vander Vusse GJ and Glatz JF: New insights into long-chain fatty acid uptake by heart muscle: A crucial role for fatty acid translocase/CD36. Biochem J 367: 561-570, 2002.
6. Griffin E, Re A, Hamel N, Fu C, Bush H, McCaffrey T and Asch AS: A link between diabetes and atherosclerosis: Glucose regulates expression of CD36 at the level of translation. Nat Med 7: 840-846, 2001.
7. Hou Y, Wu M, Wei J, Ren Y, Du C, Wu H, Li Y and Shi Y: CD36 is involved in high glucose-induced epithelial to mesenchymal transition in renal tubular epithelial cells. Biochem Biophys Res Commun 468: 281-286, 2015.
8. Lu H, Yao K, Huang D, Sun A, Zou Y, Qian J and Ge J: High glucose induces upregulation of scavenger receptors and promotes maturation of dendritic cells. Cardiovasc Diabetol 12: 80, 2013.
9. Sheedy FJ, Grebe A, RaynerK J, Kalantari P, Ramkhelawon B, Carpenter SB, Becker CE, Ediriweera HN, Mullick AE, Golenbock DT, *et al*: CD36 coordinates NLRP3 inflammasome activation by facilitating intracellular nucleation of soluble ligands into particulate ligands in sterile inflammation. Nat Immunol 14: 812-820, 2013.
10. Chen Y, Yang M, Huang W, Chen W, Zhao Y, Schulte ML, Volberding P, Gerbec Z, Zimmermann MT, Zeighami A, *et al:* Mitochondrial metabolic reprogramming by CD36 signaling drives macrophage inflammatory responses. Circ Res 125: 1087-1102, 2019.
11. Bhat A, Das S, Yadav G, Chaudhary S, Vyas A, Islam M, Gupta AC, Bajpai M, Maiwall R, Maras JS and Sarin SK: Hyperoxidized albumin modulates platelets and promotes inflammation through CD36 receptor in severe alcoholic hepatitis. Hepatol Commun 4: 50-65, 2020.
12. Yang X, Okamura DM, Lu X, Chen Y, Moorhead J, Varghese Z and Ruan XZ: CD36 in chronic kidney disease: Novel insights and therapeutic opportunities. Nat Rev Nephrol 13: 769-781, 2017.
13. Kunz A, Abe T, Hochrainer K, Shimamura M, Anrather J, Racchumi G, Zhou P and Iadecola C: Nuclear factor-kappaB activation and postischemic inflammation are suppressed in CD36-null mice after middle cerebral artery occlusion. J Neurosci 28: 1649-1658, 2008.
14. Cao D, Luo J, Zang W, Chen D, Xu H, Shi H and Jing X: Gamma-linolenic acid suppresses NF-κB signaling via CD36 in the lipopolysaccharide-induced inflammatory response in primary goat mammary gland epithelial cells. Inflammation 39: 1225-1237, 2016.
15. Sp N, Kang DK, Kim DH, Park JH, Lee HG, Kim HJ, Darvin P, Park YM and Yang YM: Inhibits CD36-dependent tumor angiogenesis, migration, invasion, and sphere formation through the Cd36/Stat3/Nf-Kb signaling axis. Nutrients 10: 772, 2018.
16. Zhao L, Zhang C, Luo X, Wang P, Zhou W, Zhong S, Xie Y, Jiang Y, Yang P, Tang R, *et al*: CD36 palmitoylation disrupts free fatty acid metabolism and promotes tissue inflammation in non-alcoholic steatohepatitis. J Hepatol 69: 705-717, 2018.
17. Hou Y, Shi Y, Han B, Liu X, Qiao X, Qi Y and Wang L: The antioxidant peptide SS31 prevents oxidative stress, downregulates CD36 and improves renal function in diabetic nephropathy. Nephrol Dial Transplant 33: 1908-1918, 2018.
18. Livak KJ and Schmittgen TD: Analysis of relative gene expression data using real-time quantitative PcR and the 2(-Delta Delta C(T)) method. Methods 25: 402-408, 2001.
19. Ruderman N, Carling D, Prentki M and Cacicedo J: AMPK, insulin resistance, and the metabolic syndrome. J Clin Invest 123: 2764-2772, 2013.
20. Ramírez E, Picatoste B, González-Bris A, Oteo M, Cruz F, Caro-Vadillo A, Egido J, Tuñón J, Morcillo MA and Lorenzo Ó: Sitagliptin improved glucose assimilation in detriment of fatty-acid utilization in experimental type-II diabetes: Role of GLP-1 isoforms in Glut4 receptor trafficking. Cardiovasc Diabetol 17: 12, 2018.
21. Palomer X, Salvadó L, Barroso E and Vázquez-Carrera M: An overview of the crosstalk between inflammatory processes and metabolic dysregulation during diabetic cardiomyopathy. Int J Cardiol 168: 3160-3172, 2013.

22. Koonen DP, Sung MM, Kao CK, Dolinsky VW, Koves TR, Ilkayeva O, Jacobs RL, Vance DE, Light PE, Muoio DM, *et al*: Alterations in skeletal muscle fatty acid handling predisposes middle-aged mice to diet-induced insulin resistance. Diabetes 59: 1366-1375, 2003.
23. Abumrad NA and Goldberg IJ. CD36 actions in the heart: Lipids, calcium, inflammation, repair and more? Biochim Biophys Acta 1861: 1442-1449, 2016.
24. Han L, Yang Q, Li J, Cheng F, Zhang Y, Li Y and Wang M: Protocatechuic acid-ameliorated endothelial oxidative stress through regulating acetylation level via CD36/AMPK pathway. J Agric Food Chem 67: 7060-7072, 2019.
25. Li W, Febbraio M, Reddy SP, Yu DY, Yamamoto M and Silverstein RL: CD36 participates in a signaling pathway that regulates ROS formation in murine VSMCs. J Clin Invest 120: 3996-4006, 2010.
26. Liang E, Liu X, Du Z, Yang R and Zhao Y: Andrographolide ameliorates diabetic cardiomyopathy in mice by blockage of oxidative damage and NF-κB-mediated inflammation. Oxid Med Cell Longev 2018: 9086747, 2018.
27. Morgan M and Liu Z: Crosstalk of reactive oxygen species and NF-κB signaling. Cell Res 21: 103-115, 2011.
28. Frati G, Schirone L, Chimenti I, Yee D, Biondi-Zoccai G, Volpe M and Sciarretta S: An overview of the inflammatory signalling mechanisms in the myocardium underlying the development of diabetic cardiomyopathy. Cardiovasc Res 113: 378-388, 2017.
29. Febbraio M, Hajjar DP and Silverstein RL: CD36: A class B scavenger receptor involved in angiogenesis, atherosclerosis, inflammation and lipid metabolism. J Clin Invest 108: 785-791, 2001.
30. Lisa S, Winer P and Wu M: Rapid analysis of glycolytic and oxidative substrate flux of cancer cells in a microplate. PLoS One 9: e109916, 2014.
31. Day EA, Ford RJ and Steinberg GR: AMPK as a therapeutic target for treating metabolic diseases. Trends Endocrinol Metab 28: 545-560, 2017.
32. Samovski D, Sun J, Pietka T, Gross RM, Eckel RH, Su X, Stahl PD and Abumrad NA: Regulation of AMPK activation by CD36 links fatty acid uptake to β-oxidation. Diabetes 64: 353-359, 2015.
33. Shrikanth CB and Nandini CD: AMPK in microvascular complications of diabetes and the beneficial effects of AMPK activators from plants. Phytomedicine 24: 152808, 2018.
34. Glatz JFC, Luiken JJFP and Nabben M: CD36 (SR-B2) as a target to treat lipid overload-induced cardiac dysfunction. J Lipid Atheroscler 9: 66-78, 2020.
35. Li Y, Yang P, Zhao L, Chen Y, Zhang X, Zeng S, Wei L, Varghese Z, Moorhead JF, Chen Y and Ruan XZ: CD36 plays a negative role in the regulation of lipophagy in hepatocytes through an AMPK-dependent pathway. J Lipid Res 60: 844-855, 2019.
36. Zhu Y, Qian X, Li J, Lin X, Luo J, Huang J and Jin Z: Astragaloside-IV protects H9C2(2-1) cardiomyocytes from high glucose-induced injury via miR-34a-mediated autophagy pathway. Artif Cells Nanomed Biotechnol 47: 4172-4181, 2019.
37. Ma L, Cao Y, Zhang L, Li K, Pan Y and Zhu J: Celastrol mitigates high glucose-induced inflammation and apoptosis in rat H9c2 cardiomyocytes via miR-345-5p/growth arrest-specific 6. J Gene Med 22: e3201, 2020.
38. Huang Z, Dong X, Zhuang X, Hu X, Wang L and Liao X: Exogenous hydrogen sulfide protects against high glucose-induced inflammation and cytotoxicity in H9c2 cardiac cells. Mol Med Rep 14: 4911-4917, 2016.
39. Zhao MX, Zhou B, Ling L, Xiong XQ, Zhang F, Chen Q, Li YH, Kang YM and Zhu GQ: Salusin-β contributes to oxidative stress and inflammation in diabetic cardiomyopathy. Cell Death Dis 8: e2690, 2017.
40. Kotla S and Rao GN: Reactive oxygen species (ROS) mediate p300-dependent STAT1 protein interaction with peroxisome proliferator-activated receptor (PPAR)-γ in CD36 protein expression and foam cell formation. J Biol Chem 290: 30306-30320, 2015.